Supporting Information

Lin Li[a], Lihong Shi[a, *], Jing Jia[a], Dan Chang, Chuan Dong[a], Shaomin Shuang[a,*]

[a] *Department of Chemistry and Chemical Engineering, Center of Environmental Science and Engineering Research, Shanxi University, Taiyuan, 030006, China*

*E-mail: shilihong@sxu.edu.cn; smshuang@sxu.edu.cn

Experimental

Apparatus

A JEM-2100 electron microscope (Tokyo, Japan) operating at 300 kV was employed to obtain the transmission electron microscopic (TEM) and high resolution transmission electron microscopy (HRTEM) images. Raman spectroscopy was characterized using Bruker Senterra dispersive Raman microscopy with laser wavelengths at 532 nm. X-ray photoelectron spectroscopy (XPS) data were obtained with an AXIS ULTRA DLD electron spectrometer from Shimadzu company using 300 W Al Kα radiation. The base pressure was about 3×10^{-9} mbar and the binding energies were referenced to the C1s line at 284.6 eV from adventitious carbon. Fourier Transform infrared (FT-IR) spectrum was recorded on Thermo Scientific Nicolet iS50 FT-IR Spectrometer. The UV-vis spectra of CDs were performed on a HITACHI U-2910 UV-Vis Spectrophotometer at 200–600 nm. Fluorescence spectra were operated with Hitachi F-4500 fluorescence spectrophotometer. Nanosecond fluorescence lifetime experiments were performed using a FLS 920 time-correlated single-photon counting (TCSPC) system under right-angle sample geometry. Images were obtained using a confocal laser scanning microscope (LSM880+Airyscan, Zeiss).

Measurements of fluorescence quantum yield

The relative QY (Φ) of the CDs was calculated using the equation of $\Phi_x = \Phi_{std}\, I_x\, A_{std}\, \eta^2_x / (I_{std}\, A_x\, \eta^2_{std})$. In the equation, I_x and I_{std} are the fluorescence intensities of the

CDs and the standard, and A_x and A_{std} are the optical densities (OD) of the CDs and the standard, respectively. Quinine sulfate in 0.1 M H_2SO_4 was chosen as a standard with a quantum yield Φ_{std} = 0.54 at 360 nm. η_x and η_{std} are the refractive index of the CDs and the standard, respectively. The absorbencies of all the samples in 1.0 cm cuvette were kept under 0.05 at the excitation wavelength to minimize re-absorption effects.

Real samples

To demonstrate the feasibility of the sensor in an actual sample, a tap water sample was taken and centrifuged at 8,000 rpm for 10 minutes to remove large particulate matter, followed by filtration with a 0.45 μm pore size filter membrane. 200 μL of CDs aqueous solution was added to 600 μL of a pH 7.4 PBS solution to measure the original fluorescence intensity. Then, tap water sample was spiked with Fe^{3+} standard solutions were added to the above CDs solution (final concentrations: 50, 75, and 100 μM), and the fluorescence intensity was measured. The Fe^{3+} concentration was calculated according to the linear equation.

Fluorescence imaging

HeLa cells were inoculated into 35 mm culture dish overnight. The old culture solution was removed, and the cells were incubated with 400 μg/mL CDs for 2 h, then washed with pH 7.4 PBS to remove free CDs particles, and the cells were immediately imaged under LSCM. Next, 35 μL of 0.01 M Fe^{3+} was added to the living cell system. Fluorescence imaging of cells were obtained by LSCM.

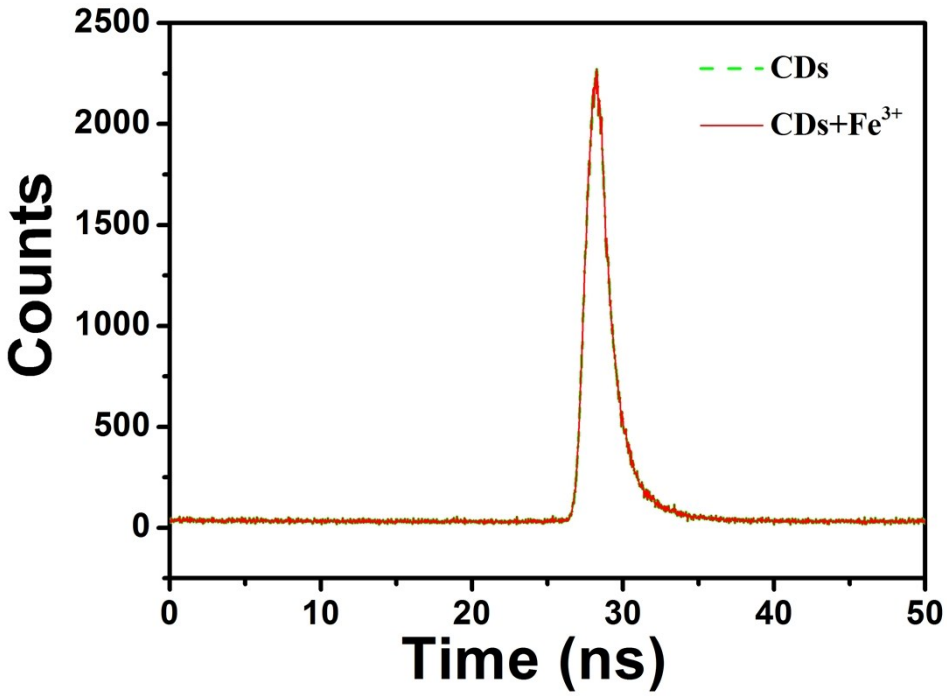

Fig. S1 Fluorescence decay curves of CDs and CDs/Fe^{3+}.

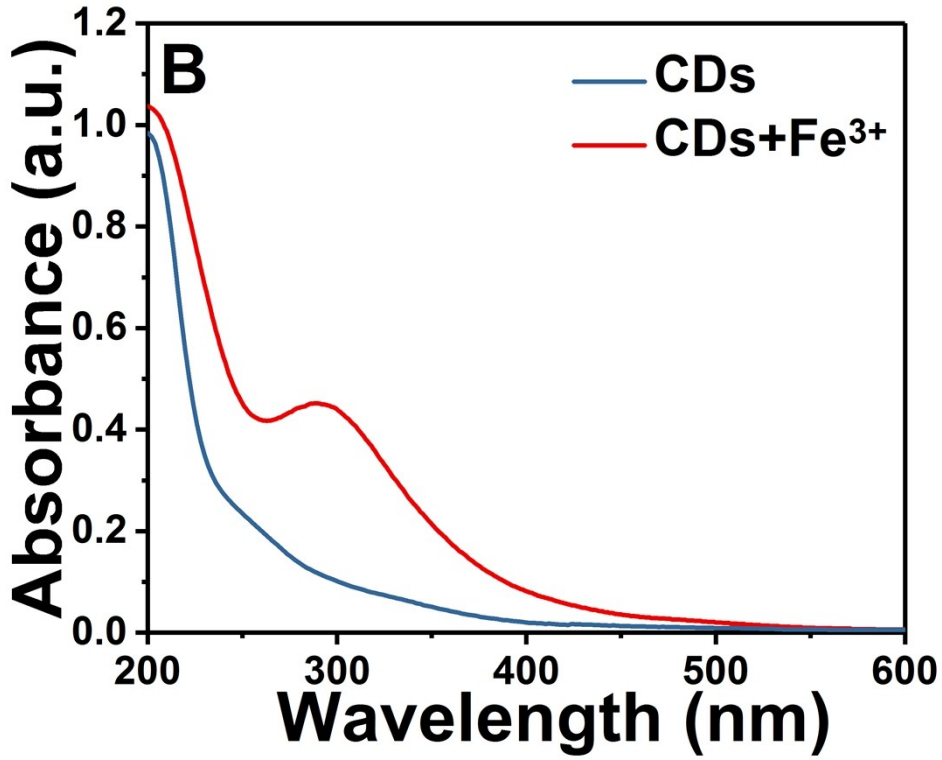

Fig. S2 The UV-vis spectra of the CDs and CDs@Fe^{3+} in aqueous solution.

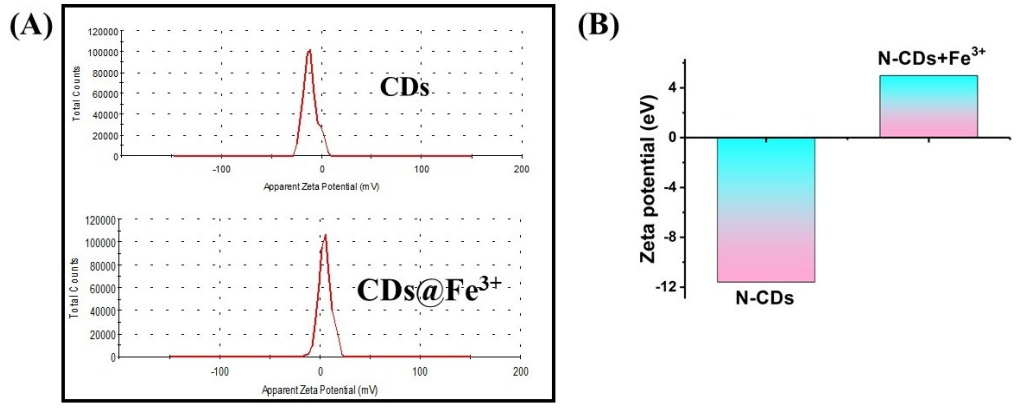

Fig.S3 Zeta potential distributions (A) and Zeta potential values (B) of the N-CDs, CDs@ Fe^{3+}.

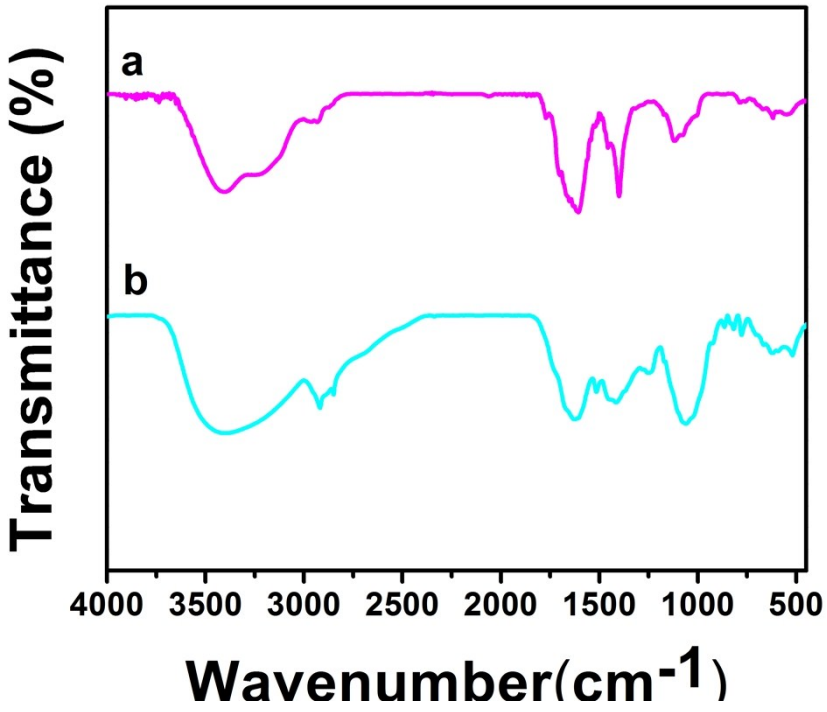

Fig.S4 FTIR spectrum of N-CDs and CDs@ Fe^{3+}.

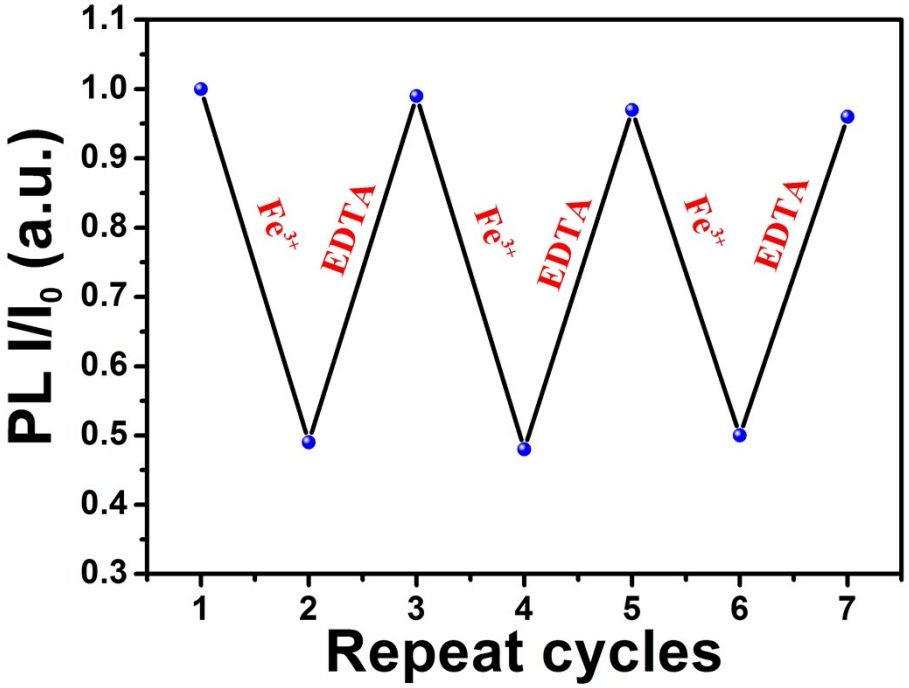

Fig. S5 Reversible cycle of CDs with Fe^{3+} and EDTA by PL intensity changes.

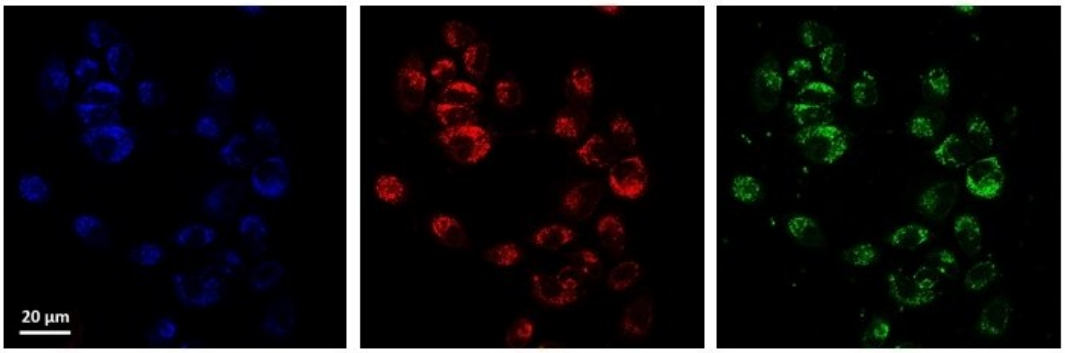

Fig. S6 CDs-stained HeLa cells at 60 s without Fe^{3+}.

Table S1 Comparison of the detection limits of Fe^{3+} from the proposed fluorescent sensor.

Precursor	Linear range	Detenction limits	Quantum yield (%)	Reference
citric acid, glycine	0-3.5 μM	0.21 μM	29.8%	[1]
Benzene boric acid ester/OPA	0.5-200 μM	0.1 μM	31.5%	[2]
Lychee waste	0.1-1.6 μM	23.6 nM	23.5%	[3]
pesticide 4-chlorophenol	0.6-26 μM	0.36 μM	22.8%	[4]
tetraethylenepentamine	0.2-600 μM	0.10 μM	26.4%	[5]
astragalus	50-250 μM	42 nM	35.6%	This work

Reference

1 R.-Q. Feng, Z.-Y. Yuan and T.-Z. Ren, *Methods Appl. Fluoresc.*, 2019, **7**, 035001.

2 H. Wu, L.-F. Pang, M.-J. Fu, X.-F. Guo and H. Wang, *Journal of Pharmaceutical and Biomedical Analysis*, 2020, **180**, 113052.

3 N. K. Sahoo, G. C. Jana, M. N. Aktara, S. Das, S. Nayim, A. Patra, P. Bhattacharjee, K. Bhadra and M. Hossain, *Materials Science and Engineering: C*, 2020, **108**, 110429.

4 Y. Wang, Y. Man, S. Li, S. Wu, X. Zhao, F. Xie, Q. Qu and W.-S. Zou, *Spectrochimica Acta Part A: Molecular and Biomolecular Spectroscopy*, 2020, **226**, 117594.

5 H. Yin, D. Gao, Y. Qiu, G. Yi, J. Li, Y. Dong, K. Zhang, Z. Xia and Q. Fu, *Nanoscale Adv.*, 2020, **2**, 1483–1492.